ECTI Transactions on Computer and Information Technology
Journal homepage: https://ph01.tci-thaijo.org/index.php/ecticit/
Published by the ECTI Association, Thailand, ISSN: 2286-9131

Brain Tumor Detection Through Modified Optimization Algorithm by Region-based Image Fusion

M.V. Srikanth[1], V.V.K.D.V. Prasad[2] and K. Satya Prasad[3]

ABSTRACT

This article is about the fusion of Brain images which are having different features. This article addresses the problems raised in pixel-level image fusion,such as blurring and artifacts caused by the unwanted addition of noise components in fused images. We extracted the regions of the brain image with the proposed tested optimal thresholding-based segmentation by optimizing thresholds with the proposed Sine function adapted improved Whale Optimization Algorithm (SiWOA) algorithm. We named the proposed fusion as SiWOA-FUSION. These optimal segmented regions and discrete wavelet coefficients of images are fused based on interval type – 2 fuzzy rules. Finally, combined image visual quality is optimized with SiWOA by assuming the amount of the correlation of differences (ACD) as an objective function. Experiments are tested on standard benchmark databases and proved better than existing methods.

Article information:

Keywords: Image Fusion, Whale Optimization Algorithm, Interval type-2 fuzzy, Discrete Wavelet Transform

Article history:
Received: August 21, 2022
Revised: October 8, 2022
Accepted: January 21, 2023
Published: March 4, 2023 (Online)

DOI: 10.37936/ecti-cit.2023171.248604

1. INTRODUCTION

Image fusion consolidates a single image that is simpler to view than the previous more than two recorded images of the same scan or object. The objective of image fusion is to introduce additional image representations more suitable for the human visual experience, in particular in remote sensing, satellite, agricultural, industrial, and medical imaging. Imaging fusion enables various approaches for accurate treatment in the sense of diagnostic imaging to mergeIt is also useful for remote sensing, where visible light can be combined with spectral imaging bands such as infrared from conventional camera sensors. Imaging fusion can also be used for the same purposes, such as removing clouds from multi-temporary recorded satellite images, as a inpainting technique for image processing, or as occluded removal of artifacts. Based on the way two images are fused, image fusion techniques are classified into three categories like pixel level, feature level, and decision level. In the case of pixel level, any operations like arithmetic operations (addition, subtraction, multiplication, etc.,) or logical operations (AND, OR, NOT,etc.,) or transformations (both images are transformed with discrete cosine transform, discrete wavelet transform,etc.,) performed on pixels directly. Where at feature level, features are extracted from both the images with various feature extraction algorithms (principal component analysis, region-based segmentation algorithms,and deep learning algorithms). This paper focuses on feature extraction-based image fusion with deep learning algorithms. Decision-level fusion requires incorporating knowledge on a higher abstraction stage and merging the effects of multiple algorithms to generate a merged final decision. Input photos are processed for extracting details. The knowledge gathered is then paired with decisions to improve traditional meaning.

2. RELATED WORK

Pixel-level image fusion techniques: As previously stated, pixel-level image fusion techniques are widely used in remote and satellite sensing[1], medical diagnosis imaging[2], and computer vision applications[3].While the uniform approach for all image fusion activities is unlikely due to the complexity of the images to be merged, the three critical phases seen in the figures will support the majority of image fusion processes. 1. i.e.,transform image, fusion, and inversely transform the transform coefficients. The

[1] The author is with Usha Rama College of Engineering and Technology,Telaprolu, India, E-mail: sree.02476@gmail.com
[2] The author is with Gudlavalleru Engineering College, Gudlavalleru, India, E-mail: varaprasadvvkd@gmail.com
[3] The author is with Jawaharlal Nehru Technological University, Kakinada, India, E-mail: prasad_kodati@yahoo.co.in

current imaging fusion strategies can be classified into four major groups based on the embraced transformation strategy: (1) methods focused on a multi-scale decomposition, methods conducting fusion directly to the picture pixels or other areas, such as the principal component space or color strength hue saturation [4-6]. (2) methods based on a fragmented representation [7, 8], or (3) multifaceted decomposition processes, fragmented representations, a study of the central variable, and other transformations. (4) The other significant aspect that influences the fusion outcome is the fusion technique and the signal transform method [9, 10]. The fusion technique is the mechanism by which the fused picture is generated from the coefficients or pixels of the images.

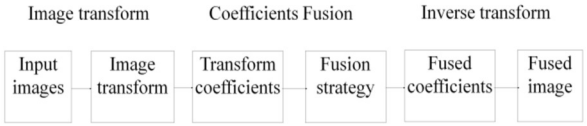

Fig.1: *Pixel-level image fusion flow.*

Decision-level Image fusion: It is a high-level fusion, offering the foundation for the decision making phase of power and management of its effects [11]. It provides the definition and rates of image fusion division and implements the most common image fusion pixel-level process. It has also developed that the pixel-level approach is better for sensor dependency, error identification, and information loss and provides optimum information than the practical level and decisions level [12].

3. METHODS AND MATERIALS

The overall proposed image fusion flow is shown in figure 2. The thermal image is down-sampled for resizing by considering one-fourth of the DWT coefficients (i.e LL bands only among four). Now, all DWT coefficients are labeled by performing a region label map (LM). These labels are assigned based on

regions/clusters obtained from segmenting the images with the thresholding-based segmentation technique. In this paper, images are segmented based on optimal thresholds which are obtained with the proposed optimization algorithm. The main aim of the fusion of the visible photos with complementary information from the thermal image is to improve the visual image. The thermal image is then used in the segmentation phase to obtain this in detail. The thermal and visual images are transformed into a frequency domain through DWT and all these coefficients from three sources are given to fusion rules for proper fusion. In this paper, these fusion rules are updated based on the fused image quality with the proposed optimization algorithm.

This process is repeated until predefined iterations or until the image quality metric is satisfied. After applying interval type-2 fuzzy rules, the fusion image is obtained by using inverse DWT. Now from the fused image and reference images, fused image metrics are measured,Based on these, metrics are optimized with the optimization algorithm used for image segmentation through image thresholding. This entire process is repeated until the expected fused image quality and expected metrics. In subsequence section, we elaborate each block thoroughly.

Discrete Wavelet Transform: As with Fourier Transform (FT), Wavelet Transform (WT) was discretized and is known as the discrete transform wavelet, which provides a significant advantage over conventional FT processes. The WT decomposes a signal into a variety of scales, representing different frequency bands, and the location of the WT can be calculated in any scale in order to detect and efficiently eliminate electric noise in a critical time characteristic. Short wavelets may be used to extract information from high-frequency components. This is valuable knowledge in order to avoid electrical noise as high-frequency variations are more likely to occur in electrical noise [13]. One can extract information from low frequencies using long-term wavelets. With high and low-frequency information, a threshold and zero frequencies can be described below the unwanted electrical noise threshold [14]. The outcome of DWT has four regions (LL, LH, HL, HH), among all, LL carries much information. Figure 3 shows the outcome of DWT of an image in three dimensional.

3.1 Segmentation

The division of images into various regions based on the pixel characteristic is the method by which artifacts or borders can be defined to simplify an image and analyze it more effectively. A variety of domains, from the film industry to pharmacy, are affected by segmentation. The program behind the green screens, for example, incorporates image segmentation to pinpoint and position it behind scenes that cannot be filmed or may be unsafe in real life. The segmentation of images is also used to monitor objects in an image series and to identify fields, such as oil reserves, in satellite images. Segmentation diagnostic uses include recognizing the damaged muscle, bone, and tissue measurements, and detecting suspected radiologist-assisted structure (CAD). One way to look at the segmentation is by clustering of pixels with such features as color, strength, or texture. Multi-level thresholding is a method in which a gray image is segmented into many different areas. For a specific image and segment the image into several regions that fit one context and several artifacts, and these techniques identify more than one threshold. The major drawback of multi-level thresholding is that, as the number of threshold levels are increased,the time for convergence also increased,and these two are proportional. So there is a need for optimization of thresholds for better segmentation.

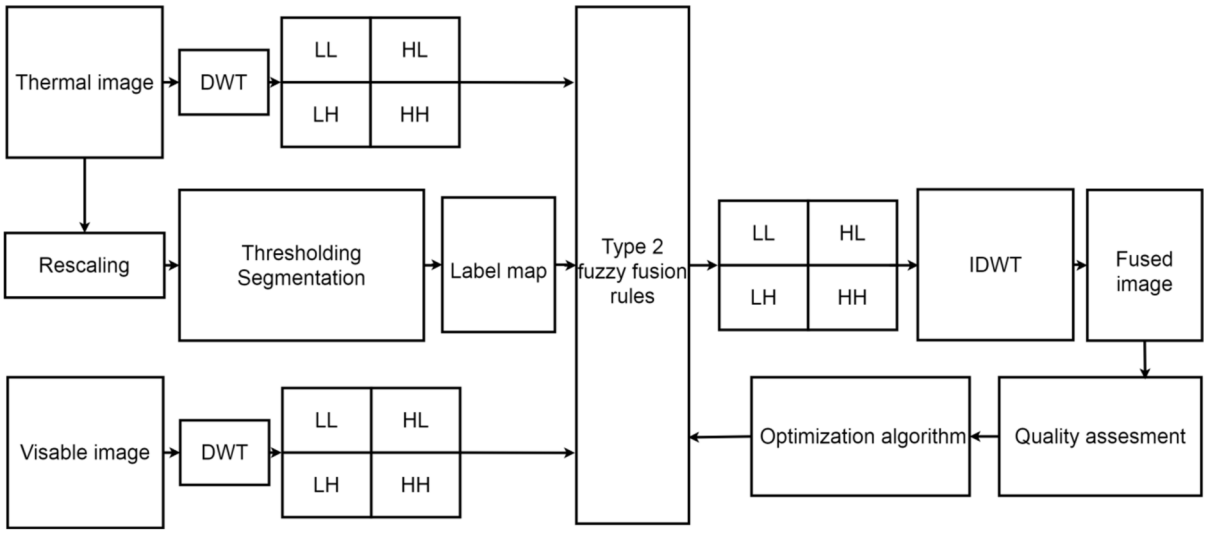

Fig.2: *Block diagram of proposed image fusion.*

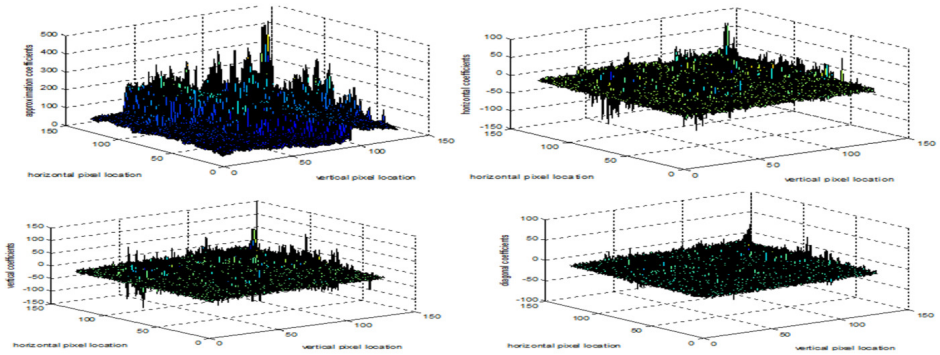

Fig.3: *Three-dimensional view of Approximation (LL), Horizontal (LH), Vertical (HL), and Diagonal (HH) coefficients of the input image.*

3.2 Overview of Sine function adapted improved WOA (SiWOA)

Numerous inspired optimization approaches for various optimization activities are being suggested. The Whale Optimization Algorithm (WOA) has been proposed by Mirjalili and Lewis, follows the skill of bumper whale hunting [15]. Yet WOA continues to hold to local optimism and premature convergence affinity. In previous research, several WOA changes to enhance the efficiency of the original WOA technique were therefore recommended. The current study indicated that the sine-adapted, enhanced WOA (SiWOA) increases WOA ability. With SiWOA, it is modified to size the step in the positioning gradation process using original WOA factor scale factors and it also uses the sine function to evaluate control parameter 'c' in the WOA process. These variations are incorporated into WOA to achieve an acceptable balance between exploitation and exploration.

The whale optimization algorithm based on the humpback whale methodology to find food was proposed by Mirjalili and Lewis. In the proximity of the water's surface, whales quest for their food. This search behavior is driven by circular bubbles. Wales use the food swimming mechanism in declining circles to get their food. Since the food location is uncertain in the quest field, the whales conclude that the new best candidate is close to the best. The rest of the whales then attempt to improve their position to the perfect situation. Two methods are the decreasing encircling method and a spiral remodeling role in the usage process of the WOA, which is regulated by the bubble-Net attack strategy. Equations [1]-[3] discuss these processes.

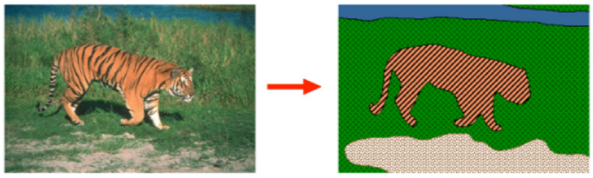

Fig.4: *Example of image segmentation.*

$$\vec{G} = |\vec{F} \times \vec{Y}^*(t) - \vec{Y}(t)| \quad (1)$$

$$\vec{Y}(t+1) = \vec{Y}^*(t) - \vec{D}\vec{G} \quad (2)$$

$$\vec{Y}(t+1) = \vec{G'}e^{lm}\cos(2\pi m) + \vec{Y}^*(t) \quad (3)$$

Where $\vec{G'} = |\vec{Y}^*(t) - \vec{Y}(t)|$ and 'k' stands for the shape of a logarithmic spiral from the ith whale to the finest wale since then. 'm' is in [-1,1] a number that's arbitrary. The vectors are different, and oscillations are vectors for adaptation that monitor and are evaluated on $\vec{D}$ and $\vec{F}$ whales location in the vicinity of food Eq. (4) and (5) ,respectively,where $\vec{Y}^*(t)$ is the current best solution until the present iteration t and $\vec{Y}^*(t)$ is the location vector. Equation (1) ensures the change of position of whales in the proximity of the finest indignation. An agent updates its location in compliance with Eq. (2) the best places to enter. Eq. (1) $\vec{F}$ alas shows the difference between the i^{th} and the best place so far achieved.

$$\vec{D} = 2\vec{d}\vec{s} - \vec{c} \quad (4)$$

$$\vec{F} = 2\vec{s} \quad (5)$$

Where $\vec{s}$ is a chosen random number from 1 to 0. In the discovery and extraction processes, parameter $\vec{d}$ decreases steadily from 2 to 0. The decrease function is ensured by the reduction of $\vec{d}$ as indicated in Eq. [5].

$$\vec{d} = 2 - t\frac{2}{ITER_{MAX}} \quad (6)$$

Where as $\vec{d}$ is the parameter for the distance control, t is the current iteration, and the limit is $ITER_{MAX}$. Proposed SiWOA uses sine to pick $\vec{d}$ as Eq. [7] for iteration.

$$\vec{d} = 2 - 2\sin\frac{t\pi}{2ITER_{MAX}} \quad (7)$$

Parameter $\vec{d}$ uses sin and cosine functions to weigh discovery and exploitation mixes. The sine function cyclic molds permitted the repositioning of an agent in some other agent's region. This approach guarantees the correct phase of exploitation and discovery. In WOA, whales are moving in the prediction step for the best solution. The best option is uncertain in the early stages. Thus, with significant steps, whales will initially shift away from the optimal location. In SiWOA, the use of scaling factors (SF) regulates the progression of whales during the search. The equations have been updated as follows:

$$\vec{G} = |\vec{F} \times \vec{Y}^*(t) - \vec{Y}(t)|/SF \quad (8)$$

$$\vec{Y}^*(t+1) = (\vec{Y}^*(t) - \vec{D}\vec{G})/SF \quad (9)$$

$$\vec{Y}^*(t+1) = (\vec{G'}e^{lm}\cos(2\pi m) + \vec{Y}^*(t))/SF \quad (10)$$

At the exploration level, scaling factors are also integrated (SF). In WOA technology, the search agent's location is reorganized into a randomly chosen search officer during the exploration. Hence in the current SiWOA process, the position of search agents is changed by scaling factors as in the following equations:

$$\vec{G} = |\vec{F} \times \vec{z_{rand}}(t) - \vec{Y}|/SF \quad (11)$$

$$\vec{Y}(t+1) = (\vec{z_{rand}}(t) - \vec{D}\vec{G})/SF \quad (12)$$

Where the scaling factor is varied as given below

$$SF = \begin{cases} 2 - t\frac{2}{ITER_{MAX}} & if\ RND < 0.5 \\ 1/(2 - \frac{t}{ITER_{MAX}}) & if\ RND \geq 0.5 \end{cases} \quad (13)$$

$$\vec{d} = 2 - \sin\frac{t\pi}{2ITER_{MAX}} \quad (14)$$

Where RND lies in the range [0, 1] and is a random value. The integration of both activity and scan factors changes the behavior of whales within the first phases of the selection process, thus increasing the process exploration capability. In the later phases, whales travel around them at regular speed with better solutions.

SiWOA is shown to attempt to scan the search area effectively to find the best solution. In the early stages, whales abruptly changed and eventually converged. The SiWOA and WOA convergence curve is contrasted for some functions in Figure 5. Only six search agents and 100 iterations are considered for a better definition of the convergence function. Figure 5 shows that SiWOA's convergence relative to WOA is increased. The improved behavior of the parameter 'c' is due to the use of sine and cosine features in SiWOA iterations compared to the existing approach used in WOA. It provides a better balance between discovery and extraction and thus increases integration to produce the best possible outcome. Scaling factors are used to adjust the scale of the phase variance. This allows SiWOA in the preliminary phase of iteration to attempt difficult areas in search space and converge rapidly. The SiWOA has high exploration capacity is attributed to an improved updating method with scaling factors.

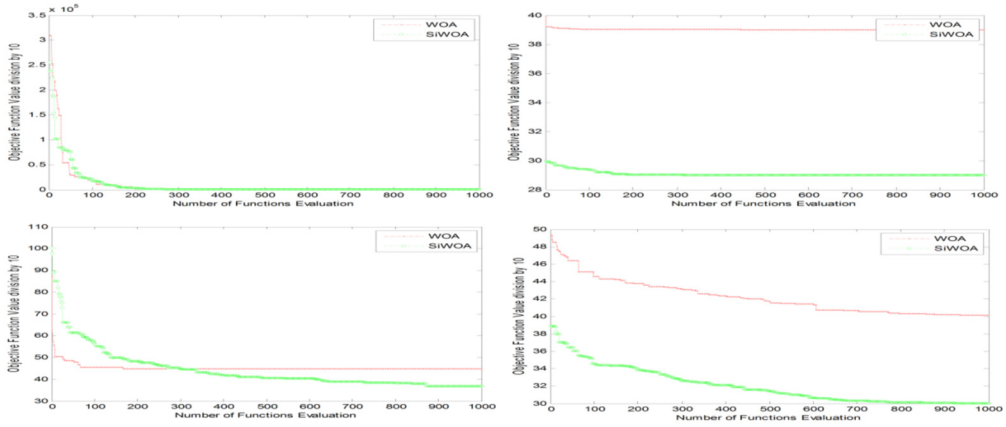

Fig.5: *Ackely graph, Alpine 1 Function, Exponential Function, Griewank.*

3.3 Amount of the correlation of differences (ACD)

To calculate the quality of the fusion images during iterations,the optimization algorithm requires quantitative value [16]. Thus, these values allow the creation of new populations. A new quality metric is created and used in this article to meet this requirement, called 'the amount of the correlation of differences.' The fused image includes data transferred from photos from the source. A pixel-by - pixel analysis of the variations between the fused image (FI) and a thermal image (TI) almost discloses the detail in the other visible embodiment (VI) and vice versa. These can be expressed as

$$\boldsymbol{FI_1 = FI - VI \& FI_2 = FI - TI} \tag{15}$$

In image fusion frameworks , it is needed to transfer the total amount of information from source images to fused images. The values obtained by correlating FI1 with VI and FI2 with TI are the similarity measures between these images. This shows how much information from VI and TI was transferred to the fused image. The number of these values (ACD) indicates how much information is transferred from the source images to the fused image. The higher the ACD value, the better the picture quality. The measure of the ACD is expressible as

$$\boldsymbol{ACD = core(FI_1 - VI) + core(FI_2 - TI)} \tag{16}$$

Where the core is the correlation coefficient between two images which is calculated with the following equation:

$$\boldsymbol{core(FI_1 - VI)} = \frac{\sum_i \sum_j (\boldsymbol{FI_1} - \overline{\boldsymbol{FI_1}})(\boldsymbol{SI} - \bar{\boldsymbol{SI}})}{\sqrt{(\sum_i \sum_j (\boldsymbol{FI_1} - \overline{\boldsymbol{FI_1}})^2)(\sum_i \sum_j (\boldsymbol{SI} - \overline{\boldsymbol{SI}}))}} \tag{17}$$

Where $\overline{\boldsymbol{SI}}$ and $\overline{\boldsymbol{FI_1}}$ are the mean values of respective images. In this paper, ACD is used as a fitness function or objective function, which is optimized with the proposed optimization algorithm. Whereas in the case of image thresholding, the objective function consider in this paper is Fuzzy entropy.For more details, please see the paper [17].

3.4 Type-2 Fuzzy Set

The Fuzzy set theory primarily addresses uncertainty-related questions. However, since traditional fuzzy set membership functions of type-1 are defined, minimizing ambiguity effects is difficult when utilizing any algorithm and membership feature. For functional implementations, the membership function is typically empirically founded on experience with a significant degree of subjectivity-a generic Fuzzy set was suggested by Zadeh to resolve the issues mentioned above, i.e., category 2 Fuzzy set. The relationship between the membership feature and entity is fuzzy and uncertain in a second-form Fuzzy set. Hence, a type-2 fuzzy collection will define the fuzzy uncertainty membership function, and the uncertainty components.

$$B = \{((y,u), \mu_B(y,u)) | \forall y \in Y, \forall u \in Ky \subseteq [0,1]\} \tag{18}$$

Where B corresponds to a type-2, μB(y, u) is referred to as the 0-alternative μB(y, u)-allocating feature of the type-2. Ky denotes the μB(y′,u) main membership feature while the Y = y′ secondary membership feature. Thus the difficulty of the type 2 fuzzy set, in which more calculations are needed, is higher than that of type 1. The question comes where secondary engagement functions are regarded.Generalized flushing type-2 collection is sometimes used for functional implementations, such as the flushing type-2 interval range [18]. In Fuzzy set type-2, the membership of the organization is specified as

$$B = \{((y,u), 1) | \forall y \in Y, \forall u \in Ky \subseteq [0,1]\} \tag{19}$$

An alternative type-2 fuzzy set is defined as (with the help of membership functions of type-1)

$$B = (y, \mu_M(y), \mu_V(y))|\forall y \in Y \\ \mu_M(y) \leq \mu(y) \leq \mu_V(y)|u \in [0,1] \quad (20)$$

Where μ(y) denotes an initial membership function of type-1, B is the interval type-2 fuzzy set, and μ_M (y) and μ_V (y) is the upper and lower membership functions with respect to upper and lower envelopes of the interval membership function (type-2) and fuzzy set type-1 membership function can be obtained. Practically a pair to characterize reciprocal parameters ,i.e.

$$\mu_M(y) = [\mu(y)]\alpha, \mu_U(y) = [\mu(y)](1/\alpha) \quad (21)$$

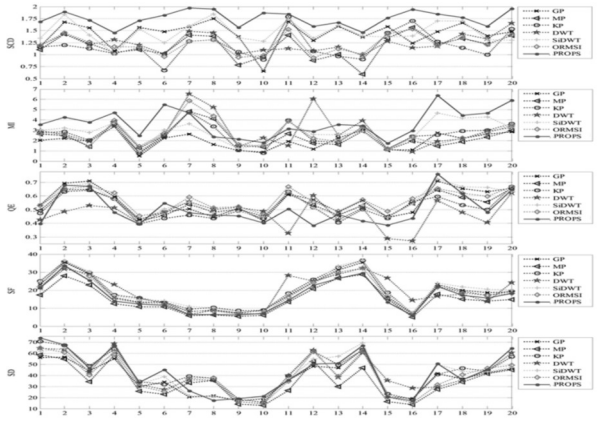

Fig.6: *Graphical view of measuring metrics [16].*

Where α is a textual shield that is naive ($\alpha \geq 1$),with $\alpha \in [1,2]$, strong performance can be achieved. The footprint of ambiguity (FOU) can be expressed by comparing the fuzzy set type-1 and the fuzzy set type-2 [19]. The form of type-2 fuzzy set used in literature is defined by the term FOU, thus FOU gives the distribution at the top of the shaded field.

Algorithm 1: Workflow of proposed image fusion
Step 1: To get the LM regions, re-dimension the thermal image to one-fourth of the size and then split the result into the default number of areas (NR) using the
Step 2: Now apply DWT on both thermal and visible images to get frequency domain coefficients
Step 3: Divide all sub-bands into regions about the LM.
Step 4: Fuse all these three input components based on type 2 Fuzzy fusion rules
Step 5: The fused image is in the frequency domain,and to get the time domain, apply inverse DWT.
Step 6: For the better visual quality of the fused image, now optimize the combined image by optimizing ACD with the proposed optimization algorithm.
Step 7: Repeat steps 4–6 until the quality of the fused image is the satisfactory or the maximum number of iterations.

3.5 Fusion Rule

Let's say two images, M and R are to be combined. After efficient segmentation of both images, their respective segmented regions are represented as $\boldsymbol{M : \{S^M_{p,q}\}}$ and $\boldsymbol{R : \{S^R_{p,q}\}}$. Where p and q represent the segmented regions and their respective pixel locations. The fusion rules play an essential part in the success of the proposed segmentation method. The previously suggested rules for image fusion are sensitive to high -frequency noise, i.e., borders, area boundaries, and textures [20].Still this paper presents a type 2 fuzzy set that takes local and global image knowledge. $\mu()$ membership function form is offered as

$$\boldsymbol{\mu^I_{p,q}(i.j) = \frac{1}{1 + |\frac{s^I_{p,q}(i,j) - c}{a}|^2}} \quad (22)$$

Where I = (M, R) and (i, j) show the location of segmented images. Here, c is the average of $(\boldsymbol{s^I_{p,q}})$ and 'a' is the minimum of $(\boldsymbol{s^I_{p,q}})$. Next, at each position of the membership function, lower and upper membership functions μ_L (x) and μ_U (x) are calculated as follows:

$$\begin{cases} \boldsymbol{\mu^{l,p,q}_L(x,y) = [\mu^I_{p,q}(i,j)]^{\alpha}} \\ \boldsymbol{\mu^{I,p,q}_U(x,y) = [\mu^I_{p,q}(i,j)]^{1/\alpha}} \end{cases} \quad (23)$$

Fuzzy set output is calculated based on fuzzy entropy, a substantial fuzzy entropy value indicates the most robust fuzzy set, and a weak fuzzy entropy value means wicked fuzzy set [21]. Hence a higher fuzzy entropy value contributes to stronger laws for image fusion.

4. RESULTS AND DISCUSSIONS

The performance of the proposed method is evaluated by performing experiments on five pairs of images related to different brain diseases. In Set-A, CT and T2- Weighted MR images of brain tumor related to neoplastic disease. In Set-B, CT, T2-Weighted MR images of brain stroke due to cerebrovascular disease. Set-C, depicts the T1-Weighted MR and T2-Weighted MR images of the brain related to Alzheimer's condition.Set-D, describes the T1-Weighted MR and T2-Weighted MR images of the brain related to fatal illness, while Set-E, represents the CT, T1-Weighted MR brain images due to sarcoma disease. The medical images used in the research were obtained from https://www.imagefusion.org/ and http://www.med.harvard.edu/ aanlib/home.html. All the simulations are performed on HP Compaq LE1902X personal computer with Matlab version 2016a.

4.1 Measuring parameters

Standard deviation (STD): The gray contrast value in the composite image is the standard deviation. The fused image should be sharply contrasting at the stage where the approximate S is small. When p(k) is a gray level k likelihood, and km is the mean of k.

$$\mathrm{STD} = \sqrt{\sum_{K=0}^{J-1}(k-k_m)^2 p(k)} \tag{24}$$

Structural similarity index (SSIM): The structural similarity index is used to measure the resemblance or closeness between two images. Comparing a given image with the other, it is used to analyze accuracy. This is regarded as being of outstanding consistency. It is the updated edition of the standardized index of image efficiency. Find D1=$(m_1N)^2$ and D2=$(m_2N)^2$ as the two variables that will balance the division by having the denominator low. N stands for vector dynamic range prices. The standard m1 and m2 values are 0.01 and 0.03, respectively. If the fused image is 'f' and the reference image is r.

$$SSIM = \frac{(2r2f + D1)(2r2f + D2)}{(2r2f + D1)(2r + 2f + D2)} \tag{25}$$

Mutual information (MI): Mutual information is used as a metric for recognizing success in multimodal fusion. When the MI is strong then it means that parental image detail is limited by the merged frame. Let p(m), p(n) is the median probability distribution function of both images; p(m, n) is the sum of the combined probability distribution.

$$MI(m,n) = \sum_{m\in M}\sum_{n\in N} p(m,n)\log\left(\frac{p(m,n)}{p(m)p(n)}\right) \tag{26}$$

Where M and N are the numbers of rows and columns of both images.

Entropy: The quantity of information that the image comprises is known as. It can be used for calculating the accuracy of the image fused from the output. The entropy will be established if the pixel-level likelihood density (p) is established. If the entropy is greater, then fusion is effective [21].

$$Entropy = -\sum_{i=0}^{K-1} p(mi)\log p(mi) \tag{27}$$

Edge-based similarity measure ($Q^{AB/F}$): It can be used to calculate the dimensions of the boundaries of a fused Photograph. Q's value for a good-quality fused image is equivalent to 1. Various methods are added to get the image's edge knowledge,such a basic algorithm for edge detection, local gradients, and much more [21]. It is determined with the equation below.

$$Q^{AB/F} = \frac{\sum_{i=1}^{x}\sum_{j=1}^{y} Qa(i,j)Wa(i,j) + Q(i,j)Wb(i,j)}{\sum_{i=1}^{x}\sum_{j=1}^{y} Wa(i,j) + Wb(i,j)} \tag{28}$$

Where $Qa(i,j) = Qa(x,y)Qa\alpha(x,y), Qb(i,j) = Qb(x,y)Qb\alpha(x,y)$

Correlation coefficient (CC): Using this function, the closeness between the reference image and the fused image is determined. If the reference image and the fused image are similar,then the coefficient of similarity is almost equal to 1. If there is an actual discrepancy between the fused image and the reference image, then the correlation coefficient value would be less than 1.

$$C = \frac{\sum_{i=1}^{j}(m_i - M)}{\sqrt{\sum_{i=1}^{j}(m_1 - M)^2 \sum_{i=1}^{j}(n_i - N)^2}} \tag{29}$$

Where M and N are the mean values of corresponding images.

4.2 Experiments on CT/MRI Image Fusion

Neoplastic disease: Neoplastic diseases are conditions that cause tumor growth. It is the kind of tumor due to the extreme development of cells in the brain. They can be benign or malignant. Benign tumors are non-cancerous and grow slowly, and spread less to other organs. Malignant tumors are cancerous and can spread to other tissues or organs. If not detected in the early stage, it may be life-threatening. Identifying such kind of growth at an early stage, may not lead to cancer. If such kind of growth is malignant, it will spread to all other parts of the brain quickly and lead to cancer. From figure 7, such type of tumor growth is identified better with the proposed algorithm as compared to others and table 1 shows the performance of the proposed algorithm in FSIM, SSIM, Entropy, PSNR, $Q^{AB/F}$, and MI.

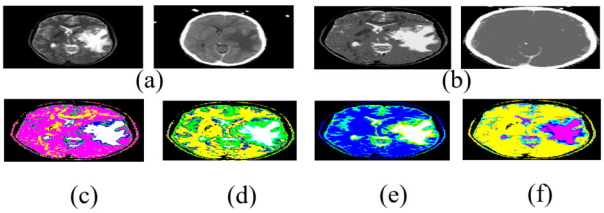

Fig. 7: *a) input images b) Segmented images: Fused images c) with PSO d) with QPSO e) with HBMO f) with Proposed.*

Cerebrovascular disease: Cerebrovascular disorder applies to conditions that may induce stroke and disrupt blood supply across the brain. The most critical risk factor for stroke and cerebrovascular disorder is hypertension (high blood pressure). This illness, is induced fatally or briefly by any of the factors such

Table 1: *Set–A: Neoplastic disease.*

Method	FSIM	ENTROPY	PSNR	SSIM	STD	$Q^{AB/F}$	MI	CC
PSO	0.893427	21.064733	34.32786	0.91319	0.189056	0.620952	3.23917	0.62095
QPSO	0.956501	21.109136	34.36472	0.914872	0.206056	0.663134	3.28259	0.66313
HBMO	0.958995	21.134748	34.38426	0.934355	0.234453	0.683590	3.28660	0.68359
Proposed	**0.993939**	**21.377371**	**34.63737**	**0.999392**	**0.494943**	**0.838382**	**3.67473**	**0.83838**

Table 2: *SET-B:CerebrovascularDisease.*

Method	FSIM	ENTROPY	PSNR	SSIM	STD	$Q^{AB/F}$	MI	CC
PSO	0.991425	22.640391	34.39331	0.94834	0.137244	0.594891	3.30639	0.59489
QPSO	0.960303	22.679535	34.58154	0.949456	0.152098	0.604217	3.34325	0.60422
HBMO	0.942479	22.689466	34.58518	0.953553	0.183669	0.683029	3.34592	0.68303
Proposed	**0.989212**	**22.939291**	**34.94944**	**0.993939**	**0.193939**	**0.839393**	**3.67373**	**0.83838**

as ischemia, brain field, excessive loss, and presence of more than two blood vessels in pathological processes. This involves aneurysms, vertebral stenosis, carotid stenosis and stroke, intracranial stenosis,and vascular malformations. Many diseases can be avoided if medicine and lifestyle are improved. Blood thinners and other modalities are used for treating strokes, including surgery. Figure 8 indicates the success of the proposed algorithm in the visual output, and table 2 indicates more potent in all proposed calculated parameters. Figure 8 shows the effectiveness of the proposed algorithm in visual quality and table 2 shows in all measured parameters proposed is better.

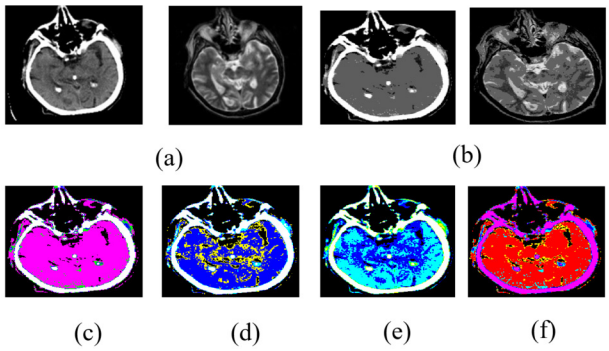

Fig.8: *a) input images b) Segmented images: Fused images c) with PSO d) with QPSO e) with HBMO f) with Proposed.*

Alzheimer's disease: Alzheimer's disease is an irreversible, progressive brain disorder that slowly destroys memory and thinking skills, eventually the ability to carry out even simple tasks. It usually appears first at the age of mid-60. There is no cure for this disease, but treatment can help slow the progression of the disease and improve quality of life. In general, this disease is diagnosed by testing metal stability manually with or by eye tracing test or by MRI scan, or by CT scan. A slight structural difference in the brain leads to disease, so identifying such kind of small difference is a big task for the researchers. In this paper, MRI and CT scan images are fused for better identification of small differences in brain which leads to early diagnosis of Alzheimer's.T1-Weighted MR image of 70 year older man and T2-Weighted MR images of 73 year old man are considered for performance test of the proposed method. The qualitative result of the proposed algorithm is well explained in figure 9. From the figure, the visual quality of Alzheimer's disease is better in the proposed as compared with other algorithms. The quantitative result of the proposed is shown in table 3. It shows superiority in all aspects.

Fatal disease: A fatal disease has no cure and ultimately results in the death of the patient. Death can occur within a few hours to several years, depending on the disease. Some examples of fatal diseases include cancer, severe heart disease, AIDS, dementia, etc. As there is no cure, the patients can only be given supportive and palliative treatment. In this paper, Pick's disease is considered a fatal disease. Pick's disease is a rare disease that leads to loss of memory, reduction in thinking levels, remembering the language, and abnormal behavior of human beings. The reason is some minor damage to brain tissues. This can be identified by fusing CT and MRI images which was successfully done with the proposed method,and comparing the results with other soft-computing techniques. Table 4 and figure 10, depicts the proposed method's effectiveness in fusing the images.

Sarcoma disease: Sarcoma is a malignant tumor, a rare kind of cancer. Sarcomas grow in connective tissue cells, for example, fat, blood vessels, nerves, bones, muscles, and cartilage. They are treated by surgery to remove the tumor and radiotherapy and chemotherapy. Sarcomas are usually incurable and can be deadly. From figure 11, the visual fused image quality obtained with SiWOA is far better than the fused images obtained with PSO, QPSO,and HBMO. The green color regions in figure 7(f) show the tumor affected areas which are top highlighted with proposed SiWOA. The proposed method is better not only in visual quality but also in other fusion measuring parameters, as shown in table 5.

From the above discussions, results,and experiments, it is found that the proposed SiWOA gives an advanced amount of mutual information (MI) by im-

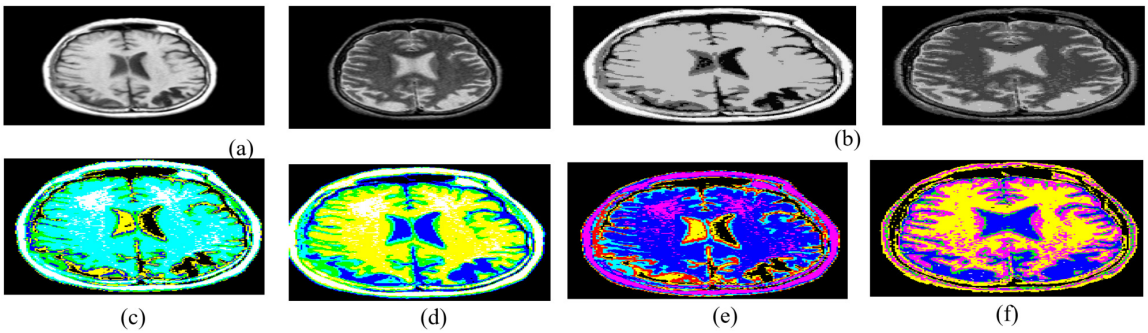

Fig.9: *a) input images b) Segmented images: Fused images c) with PSO d) with QPSO e) with HBMO f) with Proposed.*

Table 3: *Set–C : Alzheimer's disease.*

Method	FSIM	ENTROPY	PSNR	SSIM	STD	$Q^{AB/F}$	MI	CC
PSO	0.336717	21.390594	32.82359	0.911531	0.777079	0.719411	3.0035	0.71941
QPSO	0.444859	21.405167	32.83409	0.937020	0.444859	0.720572	3.1035	0.72057
HBMO	0.660980	21.485016	32.85253	0.951837	0.660980	0.725686	3.1135	0.72569
Proposed	**0.694892**	**21.486412**	**32.87231**	**0.982387**	**0.814386**	**0.762849**	**3.1367**	**0.76287**

Table 4: *Set–D : Fatal disease.*

Method	FSIM	ENTROPY	PSNR	SSIM	STD	$Q^{AB/F}$	MI	CC
PSO	0.307900	22.177216	32.56973	0.897339	0.437479	0.742869	3.54065	0.74287
QPSO	0.437479	22.254970	32.63030	0.920576	0.833801	0.756198	3.54868	0.75620
HBMO	0.693950	22.278068	32.78759	0.924099	0.307951	0.768028	3.59584	0.76803
Proposed	0.744949	22.737373	32.939391	0.993939	0.838383	0.939393	3.92929	0.93933

Table 5: *Set–E: Sarcoma disease.*

Method	**FSIM**	**ENTROPY**	**PSNR**	**SSIM**	**STD**	**$Q^{AB/F}$**	**MI**	**CC**
PSO	0.21906	21.23275	33.691	0.89593	0.24321	0.649	2.8722	0.649
QPSO	0.24321	21.25676	33.708	0.90873	0.32883	0.6583	2.8922	0.6583
HBMO	0.32883	21.39504	33.767	0.92194	0.21906	0.6615	2.8956	0.6615
Proposed	**0.83838**	**21.84848**	**33.999**	**0.99991**	**0.82828**	**0.3993**	**2.9933**	**0.8383**

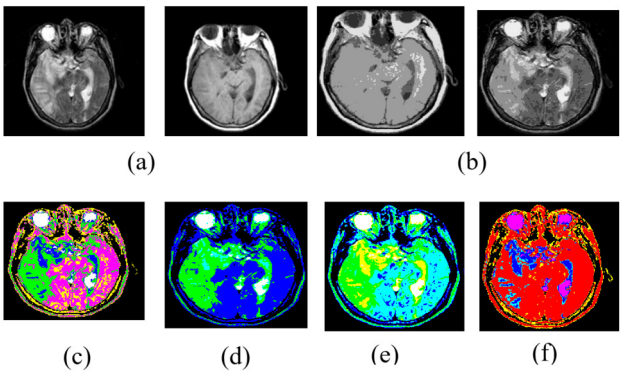

Fig.10: *a) input images b) Segmented images: Fused images c) with PSO d) with QPSO e) with HBMO f) with Proposed.*

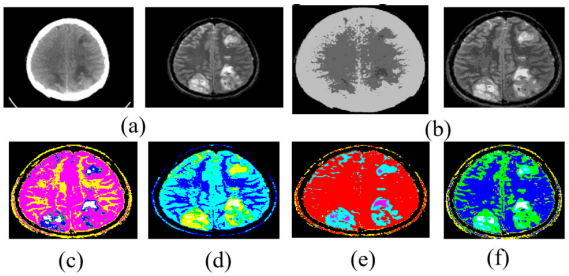

Fig.11: *a) input images b) Segmented images: Fused images c) with PSO d) with QPSO e) with HBMO f) with Proposed.*

age thresholding and Scale-Invariant Feature Transform. The experimental results show that the proposed fusion technique has significant quantitative improvement over that of the existing fusion techniques. This fusion algorithm is tested for medical imaging applications, and is also well suited for other applications like remote sensing and the developement of the region of an area. The proposed technique can be used for satellite imaging applications such as weather forecasting, forest degradation and object tracking. The proposed algorithm overcomes the limitations of PSO, QPSO, and HBMO.

5. CONCLUSIONS

Two MRI images are merged in this paper to help identify diseases such as neoplastic disease, cerebrovascular disease, Alzheimer's disease, fatal disease and sarcoma disease. The two images are segmented by assuming Fuzzy entropy as an objective function based on 2-D histogram with SiWOA. It is used to get optimum thresholds for better segmentation. The segmented regions of both images are extracted using the Scale Invariant Feature Transform (SIFT), and both images are fused based on Fuzzy set fusion laws of type-2 interval. From the experiments, the proposed algorithm is better than other algorithms in terms of visual quality for diagnosing diseases and better in terms of mutual knowledge, Edge-based similarity measurement, and correlation coefficient.

References

[1] G. Vivone et al., "A Critical Comparison Among Pansharpening Algorithms," in *IEEE Transactions on Geoscience and Remote Sensing*, vol. 53, no. 5, pp. 2565-2586, May 2015.

[2] A. P. James and B. V. Dasarathy, "Medical image fusion: A survey of state of the art," *Information Fusion*, vol. 19, pp. 4-19, Sep. 2014.

[3] Y. Liu, L. Wang, J. Cheng, C. Li and X. Chen, "Multi-focus image fusion: A Survey of state of the art," *Information Fusion*, 64, vol. 71-91, Dec. 2020.

[4] C. Hessel and J. -M. Morel, "An extended exposure fusion and its application to single image contrast enhancement," in *The IEEE Winter Conference on Applications of Computer Vision*, pp. 137-146, 2020.

[5] T. Li and Y. Wang, "Biological image fusion using NSCT based variable-weight method," *Information Fusion*, vol. 12, no. 2, pp. 85-92, 2011.

[6] S. Maqsood and U. Javed, "Multi-modal medical image fusion based on two-scale image decomposition and sparse representation," *Biomedical Signal Processing and Control*, vol. 57, 101810, Mar. 2020.

[7] Q. Zhang, Y. Liu, R. S. Blum, J. Han and D. Tao, "Sparse representation based multi-sensor image fusion for multi-focus and multi-modality images: A review," *Information Fusion*, vol. 40, pp. 57-75, Mar. 2018.

[8] K. Wang, G. Qi, Z. Zhu and Y. Chai, "A novel geometric dictionary construction approach for sparse representation based image fusion," *Entropy*, vol. 19, no.7:306, 2017.

[9] H. R. Shahdoosti and H. Ghassemian, "Combining the spectral PCA and spatial PCA fusion methods by an optimal filter," *Information Fusion*, vol. 27, pp. 150-160, Jan .2016.

[10] Z. Zhu, H. Yin, Y. Chai, Y. Li and G. Qi, "A novel multi-modality image fusion method based on image decomposition and sparse representation," *Information Sciences*, vol. 432, pp. 516-529, Mar 2018.

[11] M. K. Abd Ghani, M. A. Mohammed, N. Arunkumar, S. A. Mostafa, D. A. Ibrahim, M. K. Abdullah, and M. A. Burhanuddin, "Decision-level fusion scheme for nasopharyngeal carcinoma identification using machine learning techniques," *Neural Computing and Applications*, vol 32 no.3, pp. 625-638, 2020.

[12] S. Liu et al., "Multi-Focus Color Image Fusion Algorithm Based on Super-Resolution Reconstruction and Focused Area Detection," in *IEEE Access*, vol. 8, pp. 90760-90778, 2020.

[13] M. Bitenc, D. S. Kieffer and K. Khoshelham, "Evaluation of Wavelet Denoising Methods for Small-Scale Joint Roughness Estimation Using Terrestrial Laser Scanning," *ISPRS Annals of Photogrammetry, Remote Sensing & Spatial Information Sciences*, vol. 2, pp.81-88, 2015.

[14] K. Chiranjeevi and U. Jena, "SAR image compression using adaptive differential evolution and pattern search based K-means vector quantization," *Image Analysis & Stereology*, vol. 37, no. 1, pp. 35-54, 2018.

[15] S. Mirjalili and A. Lewis, "The whale optimization algorithm," *Advances in Engineering Software*, vol. 95, pp. 51-67, May 2016.

[16] V. Aslantas, E. Bendes, R. Kurban and A. N. Toprak, "New optimised region-based multiscale image fusion method for thermal and visible images," *IET Image Processing*, vol. 8, no. 5, pp. 289-299, May 2014.

[17] M. S. R. Naidu, P. R. Kumar and K. Chiranjeevi, "Shannon and fuzzy entropy based evolutionary image thresholding for image segmentation," *Alexandria Engineering Journal*, vol 57, no.3, pp. 1643-1655, Sep 2018.

[18] J. M. Mendel and R. I. B. John, "Type-2 fuzzy sets made simple," in *IEEE Transactions on Fuzzy Systems*, vol. 10, no. 2, pp. 117-127, April 2002.

[19] Qilian Liang and J. M. Mendel, "Interval type-2 fuzzy logic systems: theory and design," in *IEEE Transactions on Fuzzy Systems*, vol. 8, no. 5, pp. 535-550, Oct. 2000.

[20] A. K. Shukla, S. K. Banshal, T. Seth, A. Basu, R. John and P. K. Muhuri, "A Bibliometric Overview of the Field of Type-2 Fuzzy Sets and Systems [Discussion Forum]," in *IEEE Computational Intelligence Magazine*, vol. 15, no. 1, pp. 89-98, Feb. 2020.

[21] Y. Yang, Y. Que, S. Huang and P. Lin, "Multimodal Sensor Medical Image Fusion Based on Type-2 Fuzzy Logic in NSCT Domain," in *IEEE Sensors Journal*, vol. 16, no. 10, pp. 3735-3745, May 15, 2016.

M. V. Srikanth is a Research Scholar, pursuing Ph. D in the field of Image Processing from Jawaharlal Nehru Technological University, Kakinada,Andhra Pradesh, India. He has been working as an Academician in the capacity of an Assistant Professor in Electronics and Communication department of Usha Rama College of Engineering and Technology, a reputed Autonomous Engineering College in Andhra Pradesh, India. Apart from regular Academia, the zeal to explore new technologies and a penchant towards pursuing research in the field of Image Processing has made him to do the research work in a governmental organization in Andhra Pradesh. His keen interests are inclined more towards Signal Processing and Embedded Systems.

V.V.K.D.V. Prasad working as a Professor and Head of the Department of Electronics & Communication Engineering, in Gudlavalleru Engineering College, an Autonomous NBA accredited College in Andhra Pradesh, India. He received Ph. D for his work in Signal Processing in 2011 from Jawaharlal Nehru technological University, Kakinada, India. His areas of Interest include Signal Processing, Electrostatics, Electromagnetic fields and Transmission lines. He developed an abstract technical trait that addresses various other fields where digitalization can be achieved. His research findings are in the methodology used, problems encountered and the practical implications of composite features and filtering coefficients in advanced filters.

K. Satya Prasad received B.Tech. (ECE) degree from JNT University, Hyderabad, Andhra Pradesh, India in 1977, M.E. (Communication systems) from University of Madras, India in 1979, Ph.D. from IIT-Madras, India in 1989. He has more than 35 years of experience in teaching and 20 years in R&D. His current research interests include Signals & Systems, Communications, Digital signal processing, RADAR and Telemetry. He worked as Professor of Electronics & Communication Engineering & Former RECTOR, JNTUK and former Pro-Vice Chancellor, KLEF. At present he is professor of ECE and Rector, Vignan's Foundation for Science, Technology and Research (Deemed to be University), Vadlamudi, Andhra Pradesh. He received patent for his research work in 2015.